



Decoding multi-frequency scale climate-dengue dynamics: An interpretable modeling framework

Zhen Zhang ^a, Shujuan Hu ^{a,*}, Jiaxuan Hu ^a, Zihan Hao ^a, Jianping Huang ^{a,b}

^a College of Atmospheric Sciences, Lanzhou University, Lanzhou 730000, China

^b Collaborative Innovation Center for Western Ecological Safety, College of Atmospheric Sciences, Lanzhou University, Lanzhou, 730000, China



ARTICLE INFO

Keywords:

Dengue fever
Climatic effect
Multi-frequency analysis
Causal inference
Automated machine learning

ABSTRACT

Dengue fever is a growing global health threat. Previous studies indicate that climate conditions drive dengue transmission. However, the mechanisms by which climate signals operate at different frequency scales remain poorly understood. Here, focusing on Singapore, we examine multi-frequency relationships between climate factors and dengue transmission. We aim to elucidate underlying mechanisms and to develop a mechanism-driven model for short-term forecasting. Correlation analysis reveals that climate impacts on dengue exhibit frequency-specific patterns, suggesting distinct pathways of influence. Building on this, causal analysis identifies the specific climate-dengue linkages at each frequency scale. Tropical Atlantic and Central Eastern Pacific SSTs drive low-frequency dengue via local precipitation and temperature. At the high-frequency scale, SSTs from the tropical Atlantic, Central Eastern Pacific, and Indian Ocean affect dengue via dew point and precipitation. At the trend scale, SSTs in the tropical Indian Ocean and tropical Atlantic drive dengue dynamics through their effects on local dew-point temperature. Leveraging these mechanistic links, we developed frequency-specific AutoML models for Singapore that accurately forecast weekly dengue dynamics, with test RMSEs of 19.64 (low-frequency), 50.67 (high-frequency), and 2.24 (trend). Together, these analyses constitute an integrated framework for multi-frequency dengue analysis and interpretable prediction modeling, offering mechanistic insights and actionable guidance to enhance disease forecasting and public health strategies.

1. Introduction

Global warming-induced thermodynamic imbalance is reshaping infectious disease transmission through climate responses at multiple scales, such as more frequent extreme precipitation, expanded heatwaves and disrupted seasonality. Vector-borne diseases are especially vulnerable (Anikeeva et al., 2024). Dengue is a typical climate-sensitive disease and has become a major global public health threat. As the fastest-spreading mosquito-borne disease in the past 50 years (Messina et al., 2014), dengue is now one of the most prevalent infectious diseases globally (WHO, 2023) and was ranked among the top ten global health threats in 2019 (Colón-González et al., 2021). Currently, 119 endemic countries and 390 million at-risk individuals face three combined pressures: climate-driven habitat expansion, accelerated viral serotype recombination and weakened control systems under globalization (Li et al., 2018; Yang et al., 2021; Bhatt et al., 2013). These factors have intensified transmission and geographical spread, as seen in 2.8 million cases

* Corresponding author.

E-mail address: hushuju@lzu.edu.cn (S. Hu).

in Latin America in 2022 and over 5 million cases with 5000 deaths worldwide in 2023 (WHO, 2023). The El Niño-associated outbreak in Brazil in 2024 set new records, showing that dengue transmission is highly sensitive to large-scale climate anomalies (Souza et al., 2024). Extreme events can affect mosquito breeding and virus replication and interact with local weather to produce nonlinear transmission patterns. These patterns highlight the need to understand how climate signals at different temporal frequencies shape dengue epidemics. To address this, models that couple multi-frequency climate information with epidemiological data are essential. Such models link global climate signals with local meteorological variability and support climate-adaptive public health strategies, including early-warning systems and targeted interventions.

Previous studies have shown that the transmission of dengue fever is influenced by various factors, including the activity and distribution of Aedes mosquitoes (Liu-Helmersson et al., 2016), human activities (Wilder-Smith and Gubler, 2008; Kraemer et al., 2019), viral activity (Kok et al., 2023), and climate and weather conditions (Damtew et al., 2023; Liu et al., 2023). Among these factors, the climate variables play a dominant regulatory role (Earnest et al., 2012; Choi et al., 2016; Nakhapakorn and Tripathi, 2005). It exerts dominant control via two pathways, at the virological level, optimal temperatures enhance viral survival and replication, whereas extremes cause inactivation (Liu-Helmersson et al., 2014; Lu et al., 2009; Xiao et al., 2014). At the vector ecology level, aedes mosquitoes, as ectotherms, are highly sensitive to meteorological conditions: temperature governs their density, survival and biting behavior, while humidity affects reproduction and biting frequency (Almeida et al., 2005; Huey and Stevenson, 1979; Reinhold et al., 2018). Local meteorological factors affect the spread of dengue fever, and large-scale climatic drivers can also regulate its spread by changing local weather conditions. For example, anomalous sea surface temperature (SST) in equatorial Pacific can, via atmospheric teleconnections, alter local meteorological conditions in the Americas and Singapore, thereby indirectly affecting the local spread of dengue fever (Lowe et al., 2014; Earnest et al., 2012; Dostal et al., 2022). Similarly, abnormal SST in the Indian Ocean can also regulate

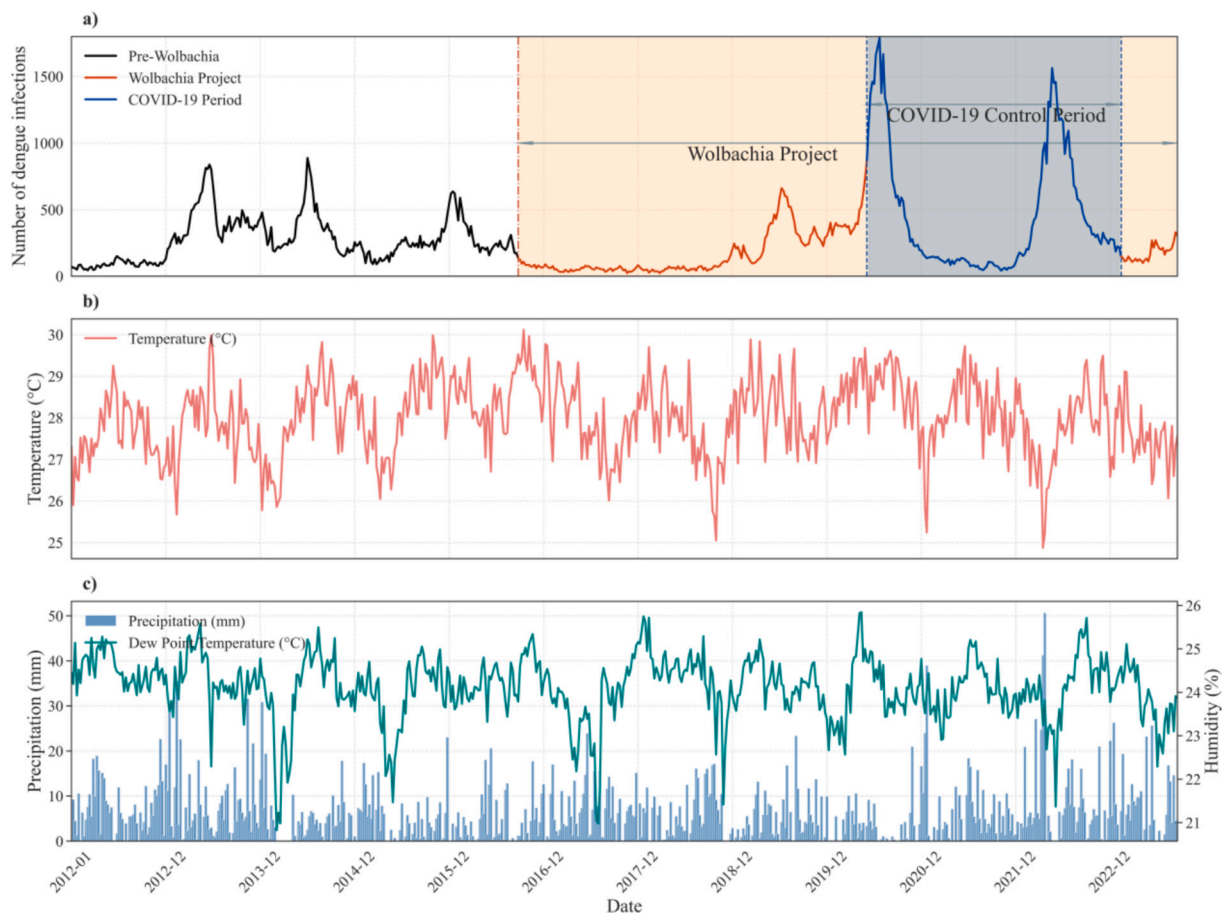


Fig. 1. Dengue infection cases and climate variables in Singapore from January 2012 to September 2023. (a) Weekly number of dengue infections. The black curve represents the pre-Wolbachia period (before week 247); the orange curves represent the Wolbachia Project period (from week 247 onwards, including the post-COVID-19 period); the blue curve represents the COVID-19 control period (weeks 439–579). The orange shaded area marks the full duration of the Wolbachia Project (week 247 to week 610), while the blue shaded area marks the COVID-19 control period (week 439 to week 579). Dashed and dash-dotted vertical lines indicate the start and end dates of these interventions. (b) Weekly mean temperature (°C). (c) Weekly total precipitation (mm, bars) and mean humidity (%) (line). (For interpretation of the references to colour in this figure legend, the reader is referred to the web version of this article.)

the temperatures in areas where dengue fever is prevalent globally, thereby affecting the spread of the epidemic (Chen et al., 2024).

Given that climate and meteorological conditions significantly affect the spread of dengue fever at multiple spatiotemporal scales, their integration into dengue prediction models is now a key focus of global environmental health. For example, Kakarla et al. (2023) applied an LSTM model integrating humidity, soil moisture, temperature, precipitation and the El Niño-Southern Oscillation (ENSO) index to forecast dengue outbreaks in India. Jayasani et al. (2021) used an LSTM-based few-shot learning framework with local meteorological variables to predict epidemics in Sri Lanka. Appice et al. (2020) used a multi-stage machine-learning model to assess temperature effects on dengue transmission. Although end-to-end data-driven models achieve high short-term accuracy, they neglect causal climate-disease mechanisms, and overlook multi-scale climate-epidemic interactions, undermining interpretability for public health governance. Spatially, abnormal SST in the tropical Atlantic and Indian Oceans can alter regional climates through distant atmospheric connections, indirectly influencing dengue spread (Gagnon et al., 2001; Yoo et al., 2006; Rong et al., 2010). Temporally, both climate variables and epidemic series show multi-frequency patterns (Van Panhuis et al., 2015; García-Carreras et al., 2022). Single-scale analyses increase the risk of spurious correlations and weak generalization. There is an urgent need for a multi-scale framework that combines climate drivers, time-frequency analysis, and epidemiological dynamics. This framework can show how large-scale climate signals affect local weather and dengue transmission and improve early warning and health-risk assessment.

Singapore has been a dengue hotspot since the 20th century, with incidence rising sharply over the past two decades. Its well-established surveillance system provides reliable case data (Struchiner et al., 2015). In this study, we develop an interpretable, multi-frequency analytical and modeling framework using Singapore as a case study. First, we decompose both the dengue incidence series and relevant meteorological variables into distinct frequency components. Second, we analyze correlations and causal links between climate factors and dengue at each scale to elucidate their mechanism of influence. Finally, we build and validate a short-term prediction model for Singapore's dengue outbreaks grounded in these relationships and physical processes. This framework of decomposition, attribution, and prediction supports epidemic control in tropical island settings. It also provides a transferable basis for early-warning systems for climate-sensitive infectious diseases worldwide.

2. Materials and methods

2.1. Data

2.1.1. Dengue case data

We obtained weekly dengue case data from the [Ministry of Health of Singapore's](https://www.moh.gov.sg) website (<https://www.moh.gov.sg>) for the period from January 2012 to September 2023, covering a total of 610 weeks (Fig. 1a). As shown in Fig. 1a), since October 2016, the government implemented a Wolbachia bacteria-based mosquito control policy (shaded orange area in Fig. 1a), which aimed to suppress Aedes mosquito reproduction by releasing male mosquitoes infected with Wolbachia bacteria, resulting in a low level of dengue cases in Singapore (Yang et al., 2021; Project Wolbachia-Singapore Consortium and Ching, 2021). During the period from 2020 to 2023 (shaded blue area in Fig. 1a), COVID-19-related movement restrictions were reported to increase exposure opportunities for Aedes mosquito bites, contributing to two consecutive dengue outbreaks (Ho et al., 2023; Lim et al., 2021). These interventions may have influenced the observed relationship between climatic factors and dengue cases. In order to focus on the effects of natural climate factors, we restricted our main analysis to data from January 2012 to October 2016 (Week 1 to Week 247), before large-scale interventions were implemented.

2.1.2. Meteorological data

This study uses hourly meteorological data from Seletar Airport and Changi Airport in Singapore, provided by [NOAA](https://www.noaa.gov), for the period from January 2011 to September 2016 (<https://www.ncei.noaa.gov/maps/hourly>). We selected temperature, liquid precipitation, and dew point temperature were selected as the primary meteorological factors. These variables are widely recognized as key drivers of dengue transmission. Previous studies have shown that warming temperatures can increase the geographic spread and epidemic potential of dengue by enhancing vectorial capacity and extending the seasonal transmission window (Liu-Helmersson et al., 2014). High mosquito biting rates and survival observed under favorable climatic conditions further underscore the role of local temperature and precipitation in facilitating dengue introduction and persistence (Almeida et al., 2005). Systematic reviews have also identified temperature, humidity, and precipitation as stable climate predictors of dengue across multiple regions (Li et al., 2018).

To ensure consistency with the weekly dengue case data from the Ministry of Health Singapore, the hourly data were converted into weekly averages, and the average of the two sites (Seletar Airport and Changi Airport) was used to represent the meteorological conditions of Singapore (Figure 1 b) and c). As illustrated in these panels, the climate variables exhibit fluctuations at multiple frequency scales, reflecting both short-term variability and longer-term trends that may influence dengue transmission. In addition, global weekly SST data from [NOAA's](https://psl.noaa.gov) Physical Sciences Laboratory (<https://psl.noaa.gov>) were obtained to analyze the lagged correlation (1–12 weeks) between global SST and dengue cases in Singapore from January 2012 to September 2016. The results indicated significant positive correlations between SST in the Indian Ocean (10°S-24°N, 55°E-138°E), the Central Eastern Pacific (0°-15°N, 100°W-140°W), and the tropical Atlantic (20°S-10°N, 4°W-50°W) and dengue infection cases in Singapore. Therefore, this study selected the average SSTs of the three marine regions as primary signals influencing Singapore's dengue epidemic.

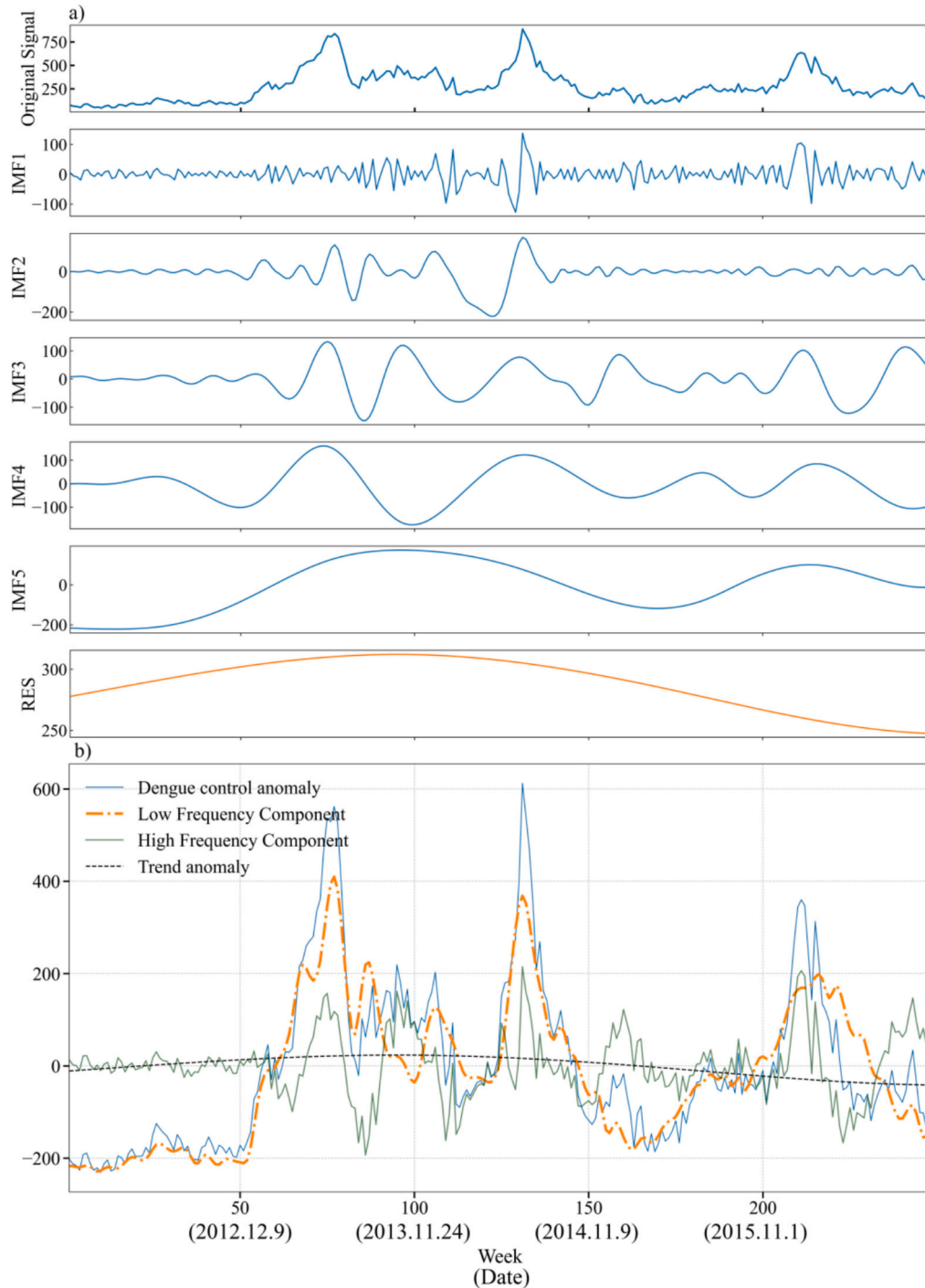


Fig. 2. Decomposition and signal extraction results of dengue fever cases in Singapore from January 2012 to October 2016. a) Decomposition results, shown from top to bottom: original signal, first to fifth intrinsic mode functions, and residuals. b) The results of different frequency components, with the blue curve representing the anomaly values of the original data, the orange curve indicating the low-frequency component, the green curve representing the high-frequency component, and the black dashed line showing the anomaly values of the trend component. (For interpretation of the references to colour in this figure legend, the reader is referred to the web version of this article.)

2.2. Methods

2.2.1. CEEMDAN algorithm for time series decomposition and signal extraction

To analyze the relationships between climate factors and dengue series at different time scales, we used the CEEMDAN algorithm (Torres et al., 2011) to decompose the raw time series of each variable, obtaining the intrinsic mode functions (IMFs) at different frequencies. CEEMDAN effectively resolves the frequency-mode mixing problem in standard EMD, decomposing signals based on their intrinsic frequency characteristics while minimizing information loss. Its specific computation process is as follows. First, multiple white noise sequences are added to the original signal, and each noisy signal is decomposed using EMD to obtain several IMFs and a residue. Then, the IMFs of all noisy signals are averaged to obtain the final IMF components, removing the noise influence. Finally, the original signal is iteratively decomposed until all components meet the local characteristics of the signal (specific computation process and parameter settings are provided in the supplementary materials, Fig. S2).

Using the CEEMDAN algorithm, each series was decomposed into several intrinsic mode functions (IMFs) and a residual. We calculated the sample entropy of each IMF to measure its complexity, where higher values indicate higher frequency. We then used the mean sample entropy as a threshold to separate high and low frequencies. IMFs with values above the threshold were summed to form the high-frequency part, and those with values below the threshold formed the low-frequency part. The residual represented the trend. This process extracted signals at different frequencies from the original data.

2.2.2. PCMCI algorithm for identifying time-delay causal relationships

We use the PCMCI algorithm to identify and quantify time-lagged causal relationships between climate variables and dengue case time series in Singapore. Assuming causal sufficiency and the Markov condition, the PCMCI algorithm first uses the PC1 algorithm (Spirtes and Glymour, 1991) to perform an initial selection of the parent node set, which includes variables associated with the target variable. Next, conditional independence tests remove spurious links and retain significant causal connections. Finally, causal graphs across different time lags are constructed from the test results. The detailed steps are provided in the supplementary materials. Additionally, we used the Python package Tigramite 5.2 to implement the PCMCI-based time-delay causal relationship identification for multivariate time series (Runge et al., 2019). However, PCMCI has several limitations. The conditional-independence tests are most powerful for linear relationships, so strong nonlinear dependencies may be missed. Its performance also degrades in very high-dimensional settings because conditioning sets grow and multiple tests reduce statistical power.

2.2.3. Automated machine learning for predictive modeling

To further understand the dynamics and patterns of how different time-scale variables influence the spread of dengue fever in Singapore under climate change, we developed short-term predictive models based on automated machine learning (Auto-ML) methods for the different frequency components of the dengue fever case series. Auto-ML automates data preprocessing, feature engineering, model selection, hyperparameter tuning, and prediction using multiple algorithms. Among the multiple Auto-ML tools available, Truong et al. (2019) found that H2O-AutoML(2023a; 2023b) exhibited the best predictive performance through multiple regression task. It can leverage multiple CPU cores and clusters for parallel processing, speeding up optimization and rapidly identifying optimal hyperparameters within preset time limits. Moreover, many of its underlying algorithms implement techniques to mitigate overfitting. For example, cross-validation in Stacked Ensemble models, dropout in Deep Learning models, and regularization penalties in Generalized Linear Models (GLM). Based on the identified relationships between different frequency variables, we used H2O AutoML for model search and hyperparameter optimization, ultimately establishing short-term prediction models for dengue fever in Singapore (For details, see: <https://docs.h2o.ai/h2o/latest-stable/h2o-docs/automl.html>).

3. Results

3.1. Decomposition and signal extraction of climate variables and dengue fever series

To investigate how climate variables at different scales influence dengue cases in Singapore, we performed CEEMDAN decomposition on the dengue fever time series, tropical Indian Ocean SST, Central Eastern Pacific SST, tropical Atlantic SST, as well as temperature, dew point temperature, and precipitation time series for Singapore over the selected period. Figure 2a) shows five intrinsic mode functions (blue) and the residual (orange) for dengue cases. Before analyzing climate impacts, we evaluated the decomposition results and identified the main dengue components using Pearson and Kendall correlations and variance contributions (Table S1).

Table S1 presents the statistical metrics of the CEEMDAN components of the dengue fever case time series. All components passed the Pearson correlation test ($p < 0.01$), but only the residual failed the Kendall test. This suggests minimal error in the CEEMDAN decomposition. Among the five intrinsic mode functions, IMF5 (with a variance contribution of 51.14 %) and IMF4 (with a variance contribution of 22.43 %) explain most variation, while the variance contribution of the residual component is only 1.94 %. Thus, IMF4–5 mainly drove epidemic dynamics from 2012–2016. Further signal extraction was performed by measuring the complexity of IMFs through sample entropy, which was then used as a selection criterion to obtain high-frequency components, low-frequency components, and residual trend components. Fig. 2b) shows the results of the extraction components of dengue fever cases in Singapore from 2012 to 2016 for different frequencies. The low-frequency component (orange dashed line) exhibits a larger amplitude and captures the peaks and valleys of the epidemic, potentially reflecting external climatic or ecological changes; the high-frequency component (green solid line) has a smaller amplitude, likely reflecting the influence of confounding factors; the residual trend

component (black dashed line) changes slowly around the mean, revealing the long-term trend.

We assessed predictability by analyzing complexity, stationarity, and randomness. Complexity was quantified using sample entropy, permutation entropy, and fuzzy entropy, while randomness was evaluated using the Hurst index and the 10th-order Ljung-Box (LB) statistic. Stationarity was analyzed through unit root tests (specific results are shown in Table S2). Entropy analysis shows highest complexity in the high-frequency component, lower in the low-frequency, and lowest in the residual. The Hurst index (where values closer to 0.5 indicate greater randomness and lower predictability) reveals that the low-frequency and residual components have relatively good predictability, while the high-frequency component is less predictable. White noise tests confirm all components are non-white sequences. Unit root tests show high- and low-frequency are stationary, while the residual has a trend. Overall, all three components are predictable, making frequency-based prediction feasible.

We also decomposed meteorological factors. For the SST of tropical Indian Ocean, Central Eastern Pacific, and tropical Atlantic, as well as the local temperature, dew point temperature, and precipitation series in Singapore, we also extracted the low-frequency, high-frequency, and trend components (the results are shown in Figs. S3–S8). SST low-frequency reflects seasonal to interannual variability, high-frequency shows weekly-monthly variability, and the trend captures long-term changes. Similarly, Singapore's temperature, dew point, and precipitation show seasonal variability at low frequency, daily variability at high frequency, and long-term change in the trend. In addition, to ensure the robustness of these decompositions, we conducted a comprehensive sensitivity analysis of CEEMDAN under different parameter settings (Figure S9), confirming that the low-frequency and trend components are generally stable across parameter choices.

In summary, we used the CEEMDAN algorithm to extract low-, high-frequency, and trend components of climate variables and dengue cases in Singapore. These components reconstruct the original signals at different frequencies and provide practical insights. Next, we analyze how climate factors affect dengue cases using these components, offering theoretical support for physically based prediction models.

3.2. Correlation analysis between multi-frequency scale components of climate variables and dengue fever series

3.2.1. Linear correlation analysis

We used Pearson correlation coefficients to examine linear relationships between dengue components and climate factors at different frequency scales (Fig. 3). The low-frequency dengue component shows significant correlations with low-frequency SSTs in three key regions and with Singapore's local temperature and precipitation. The correlation at high frequency components is weaker, likely due to the strong randomness and the influence of confounding factors. The trend component is negatively correlated with the residuals of Singapore's temperature and Indian Ocean SST. It is positively correlated with the residuals of Singapore's precipitation and Atlantic Ocean SST. These results suggest that climate modulation of dengue transmission mainly appears in low-frequency components (seasonal and interannual climate forcings) and residual trends (long-term climatic background changes).

3.2.2. Lagged correlation analysis

To identify key precursor signals for dengue prediction modeling, We analyzed lagged correlations between dengue case numbers and climate variables to identify key precursor signals (Fig. S10–S12). Using 26-week cross-correlation coefficients, we found that SST of the tropical Atlantic and Central Eastern Pacific, dew point temperature, precipitation, and temperature in Singapore significantly influence the low-frequency component of dengue cases at lags of 9, 5, 23, 1, and 1 weeks, respectively. The residual components of the dengue fever series are influenced by tropical Atlantic Ocean SST (lag 1 week), Central Eastern Pacific Ocean SST (lag 26 weeks), dew point (lag 26 weeks), tropical Indian Ocean SST (lag 1 week), precipitation (lag 1 week), and temperature (lag 1 week). The high-frequency component is influenced only by tropical Indian Ocean SST (lag 23 weeks) and Singapore dew point temperature (lag 7 weeks). These results identify the most influential climate variables at each frequency scale as key factors for multi-scale dengue prediction modeling in Singapore.

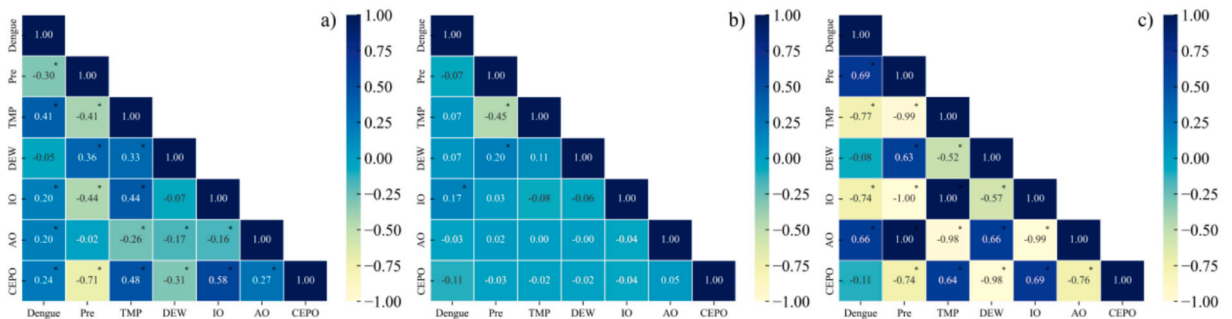


Fig. 3. Heatmap of correlation between variables: a) low-frequency components, b) high-frequency components, and c) trend components. * indicates significance at the 95 % confidence level based on the t-test.

3.2.3. Autocorrelation analysis of dengue sequence

We previously analyzed correlations between Singapore's dengue cases and climate factors at different frequency scales. Because dengue shows strong periodicity and lag effects, we performed autocorrelation analysis on the reconstructed dengue components to clarify incidence patterns and support predictive modeling (Fig. S13–S15). The results show that autocorrelation coefficients of low-frequency, high-frequency, and trend components all tail off, indicating long-period autocorrelations. However, partial autocorrelation truncation orders differ: 4 for low-frequency, 2 for high-frequency, and 1 for trend components. Accordingly, we used 1–4 week lags as autoregressive terms for the low-frequency component, 1–2 weeks for the high-frequency component, and 1 week for the trend component.

In summary, climate factors mainly affect the low-frequency and trend components of Singapore's dengue series. The decomposed dengue components themselves also show strong autocorrelation. However, correlation does not equate to causality. Thus, to further elucidate the mechanisms by which climate variables affect dengue transmission we next analyze lagged causal relationships between climate variables at different frequency scales and dengue case numbers.

3.3. Causal relationships between multi-frequency scale components of climate variables and dengue fever series

We applied the PCMCI algorithm to analyze the causal relationships between different variables with a 26-week lag (Fig. 4). We mainly investigate the causal relationship between local meteorological factors and dengue fever incidence in Singapore, and how regional SSTs indirectly influence dengue epidemics through local weather. To clearly demonstrate the cascading climate-meteorology-dengue transmission pathway, Fig. 4 omitted the connections among the three SSTs sequences and the connections among the local meteorological elements. Fig. 4a) illustrates that low-frequency SST strongly affect Singapore's precipitation and air temperature. Specifically, Central Eastern Pacific SST correlates positively with both precipitation and air temperature, whereas Atlantic SST correlates negatively with air temperature. Locally, air temperature is negatively associated with dengue case, while precipitation and dew-point temperature are positively linked. Overall, SSTs indirectly drive dengue epidemic dynamics by modulating local precipitation and temperature.

High-frequency analysis (Fig. 4b) shows that Central Eastern Pacific SST influences precipitation, air temperature and dew-point temperature in Singapore; tropical Indian Ocean SST is positively associated with air and dew-point temperatures; tropical Atlantic SST is positively associated with dew-point temperature but negatively associated with precipitation. Locally, precipitation correlates positively with dengue incidence, dew-point temperature correlates negatively, and air temperature shows no significant effect. Thus, high-frequency SSTs indirectly drive dengue epidemics by modulating local precipitation and dew-point temperature.

Trend component analysis (Fig. 4c) indicates that tropical Indian Ocean and tropical Atlantic SSTs significantly influences Singapore's climate by modulating dew-point trends, other SSTs show no notable impact. Among local meteorological trends, only dew point temperature is negatively associated with dengue incidence, while precipitation and air-temperature trends are insignificant. Thus, at the trend scale, tropical Indian Ocean SST drives dengue dynamics primarily through its effect on local dew-point temperature.

In summary, across all scales, regional SSTs modulate local meteorology, which drives dengue transmission. Both SSTs and local climate are robust precursor signals. These clear, frequency-specific causal links support predictive modelling and reveal underlying mechanisms.

In addition, Fig. 4 shows that the low-frequency and residual components of SST, local meteorological variables and dengue incidence exhibit strong autocorrelation, whereas high-frequency components display weaker autocorrelation. The PCMCI algorithm confirms that all three dengue-fever components retain significant temporal persistence (Section 3.2.3). Accordingly, predictive

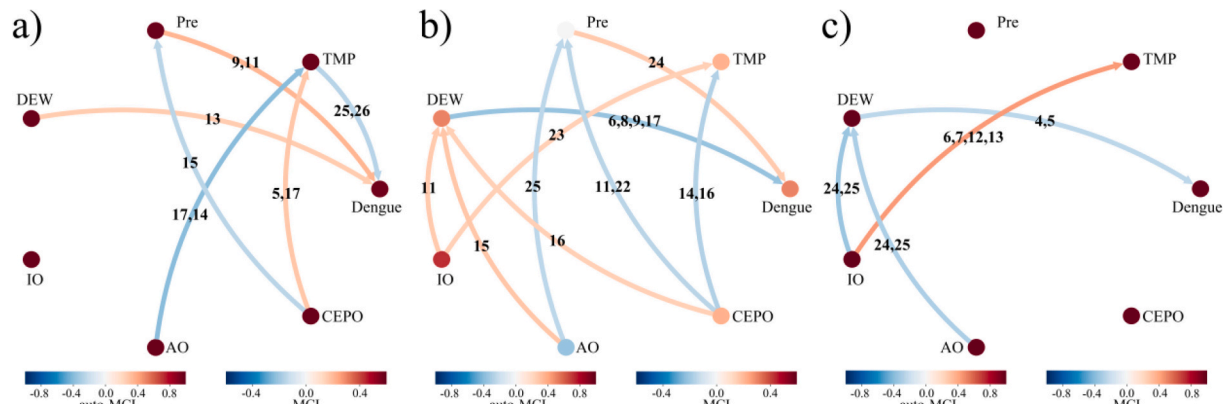


Fig. 4. Causal relationship diagram for the components: a) low-frequency component, b) high-frequency component, and c) trend component. The node colour represents the autocorrelation strength of each variable, while the arrow colour indicates the causal effect magnitude at the corresponding lag period (in weeks). Blue (red) arrows represent negative (positive) causal relationships. (For interpretation of the references to colour in this figure legend, the reader is referred to the web version of this article.)

models should include autoregressive terms to capture this memory effect.

In general, we have clarified the key meteorological factors and their corresponding causal relationships at different frequency scales that influence the development and transmission of dengue fever in Singapore. And we also estimated the 95% confidence intervals for each edge in Fig. 4 using Fisher's Z-transformation; the results are provided in the Supplementary Materials (Tables S3–S5). Furthermore, to assess the robustness of these causal relationships to CEEMDAN-related uncertainties, we analyzed the causal networks derived from decomposed components under different CEEMDAN parameter combinations (Figure S16), which confirmed the stability patterns described above. Based on this, we will use automated machine learning techniques for predictive modeling of the different frequency components.

3.4. Short-term dengue fever prediction modeling using automated machine learning based on causal relationships of multi-frequency scale components

3.4.1. Model Results

Based on the analysis of climate variables and dengue sequence at different frequencies in the previous study, we employed an automated machine learning approach to model the low-frequency, high-frequency, and trend components of dengue fever cases in Singapore, respectively. The training set and test set account for 75 % and 25 % of the total sample size, respectively. For the low-frequency component, the best model selected by automated machine learning was a stacked ensemble, with a root mean square error (RMSE) of 19.64 on the test set (Fig. 5a)). For the high-frequency component, the best model selected was a deep learning model, with an RMSE of 50.67 on the test set (Fig. 5b)). For the trend component, the best model selected was a GLM, with an RMSE of 2.24 on the test set (Fig. 5c)), see Table S6 and S7 for detailed model parameters.

To further analyze the prediction performance of the three models on the original data, we combined the training and test data from all three models to obtain the predicted values for the actual case numbers (Fig. 5d)). As shown in Fig. 5d), the predicted values closely match the actual values in the training set (from January 1, 2012, to August 16, 2015, covering 185 weeks). Similarly, the model performed well on the test set (from August 22, 2015, to September 25, 2016, covering 62 weeks). To further assess the prediction accuracy for actual case numbers, we used root mean square error (RMSE), mean absolute error (MAE), and mean absolute percentage error (MAPE) as error evaluation metrics. The specific expressions for these three metrics are as follows:

$$\text{RMSE} = \sqrt{\frac{1}{n} \sum_{i=1}^n (y_i - \hat{y}_i)^2}, \quad (1)$$

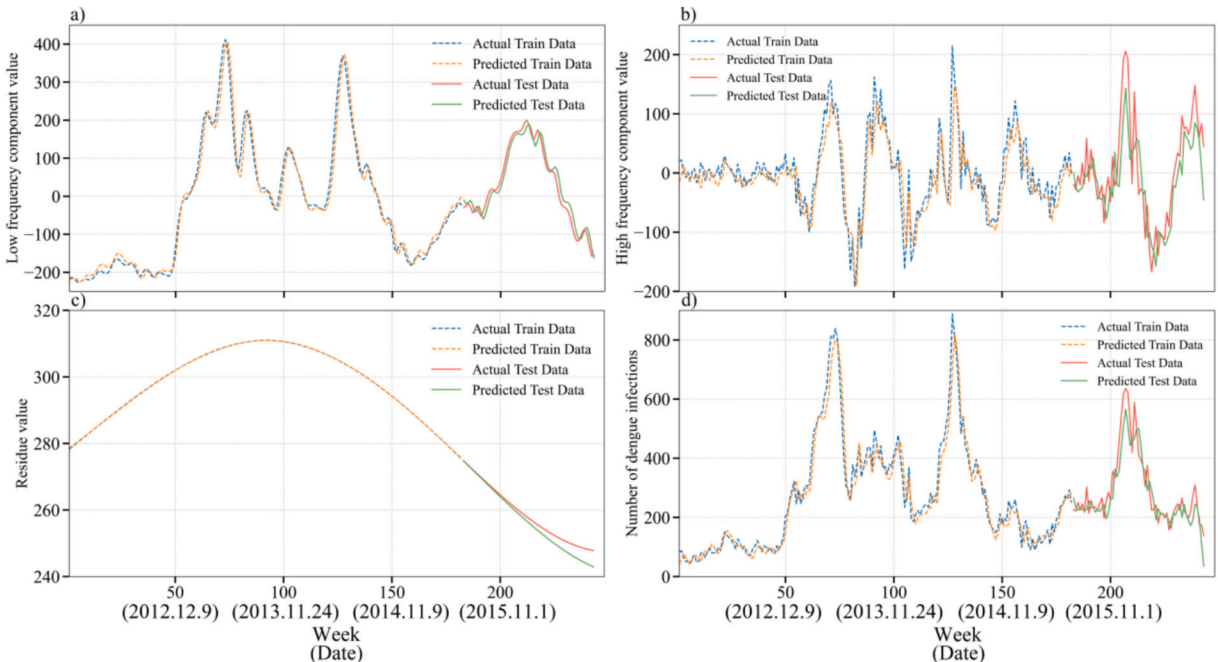


Fig. 5. Model performance for a) low-frequency component, b) high-frequency component, c) trend component, and d) reconstructed sequence. The blue dashed line represents the actual values in the training set, the orange dashed line represents the predicted values in the training set, the red solid line represents the actual values in the test set, and the green solid line represents the predicted values in the test set. (For interpretation of the references to colour in this figure legend, the reader is referred to the web version of this article.)

$$\text{MAE} = \frac{1}{n} \sum_{i=1}^n |y_i - \hat{y}_i|, \quad (2)$$

$$\text{MAPE} = \frac{1}{n} \sum_{i=1}^n \left| \frac{y_i - \hat{y}_i}{y_i} \right| \times 100\%. \quad (3)$$

Where, y_i represents the i -th actual value, \hat{y}_i represents the i -th predicted value, and n is the sample size. Smaller values of the three error metrics indicate better model performance. Upon calculation, the RMSE of the actual case number prediction model on the training set was 40.49, the MAE was 29.83, and the MAPE was 13.23 %. On the test set, the RMSE was 53.64, the MAE was 41.84, and the MAPE was 14.27 %. These results demonstrate that the approach of causal relationship analysis and multi-frequency prediction modeling is both reasonable and effective. By decomposing variables at different frequency scales, this method enables a more rational selection of predictive factors, reduces signal aliasing and interference, and optimizes models across scales. Through such multi-scale integration, the final predictions are more accurate and robust.

3.4.2. Model Residual and Sensitivity Analyses

To evaluate the potential risk of overfitting in the baseline model, we conducted residual diagnostics comparing training and test sets. The residual distributions of the training and test sets were generally similar in shape and location, with no obvious systematic bias (Figure S17 a)–c). Statistical tests also indicated no significant difference in mean residuals between training and test sets (Welch's t -test, $p = 0.15$), and a small effect size (Cohen's $d = -0.24$). Although the test-set variance was somewhat larger (Levene's test, $p = 0.004$), the predicted versus actual plots showed both sets clustered around the 45° line, supporting stable predictive performance (Table S8). These results suggest that the model maintains good generalization despite the limited sample size.

Beyond the residual diagnostics, we further examined the robustness of the modeling framework to different parameter configurations and stochasticity in the modeling process. Overall, models without algorithm exclusions tended to perform worse, while including more relevant variables generally improved both accuracy and stability. The impact of maximum search time was limited, mainly affecting models with fewer predictors, and in most cases, models using the 0.75 train-test split showed superior and more stable performance (Figures S18–S20). Specifically, we evaluated model performance across variations in training data proportion, predictor sets, algorithm exclusions, and maximum runtime using stratified random sampling of 12 model combinations for each data-splitting scheme (Table S9; Figure S21 a,b). This analysis showed that reconstructed prediction sequences captured the combined effects of parameter and predictor variations, with models trained with a 70% split producing the most stable reconstructed predictions. In addition, by iteratively refitting each frequency component 10 times under different random seeds, we quantified the variability introduced by stochasticity in the H2O modeling process (Figure S22). Despite inherent randomness, the variability across repeated runs remained small, and the reconstructed sequences consistently demonstrated stable and reliable predictive performance.

We further analyzed the impact of different CEEMDAN parameter combinations on model performance in the test set (Figures S23–S24). Overall, the Trend component was more sensitive to parameter choices, while the High-frequency component remained relatively stable. RMSE distributions for the Low-frequency and Trend components were unimodal, whereas the reconstructed sequence exhibited a bimodal distribution with peaks around 60 and 90.

4. Discussion

4.1. Physical mechanisms of climatic factors influencing dengue fever transmission at different frequency scales

To clarify the proposed analytical framework and better explain the role of different frequency-scale variables in predicting dengue fever, we need to discuss the potential physical mechanisms linking climate factors to dengue transmission, drawing on the results of causation and cross-correlation.

Since SST signals vary slowly, we focus on how SSTs from three key regions influence the low-frequency and residual components of Singapore's meteorological variables. Research shows that higher SST in the central and Central Eastern Pacific weakens the equatorial Walker circulation, suppresses the upward movement of Southeast Asian moist air, and thus warms and dries Singapore (Chang et al., 2005). SST in the tropical Atlantic, through the Gill response, excites Kelvin waves, inducing negative vorticity anomalies over the Indian Ocean, which guides cold air from higher latitudes southward, thus lowering the temperature in Singapore (Rong et al., 2010). SST in the Indian Ocean and South China Sea influences Singapore's climate by modulating the western Pacific subtropical high (WPSH) and monsoon patterns. Abnormally warm SST enhance the WPSH, suppressing convection, lowering dew point temperature in Singapore, and reducing cloud cover, which increases the shortwave radiation reaching the surface, indirectly raising the temperature in Singapore (Yoo et al., 2006). In conclusion, our framework captures how SSTs in the three key regions relate to local precipitation and temperature in Singapore, providing a reasonable mechanism explanation. As a result, the model established in this study can effectively predict dengue fever in Singapore.

In analyzing the relationship between Singapore's meteorological elements and dengue fever transmission, it was found that the variance of low-frequency components contributes significantly. Therefore, the focus is placed on the cross-correlation and causal relationships of the low-frequency components. The causal relationship between precipitation and dengue cases shows a short-term inhibitory effect, as rainfall flushes Aedes mosquito breeding sites. However, long-term effects may be positive, as water accumulation can promote mosquito breeding and transmission (Seidahmed and Eltahir, 2016). Short-term temperature increases promote

transmission by shortening the viral incubation period and increasing mosquito biting rates. In contrast, prolonged high temperatures may reduce mosquito lifespan and survival by downregulating heat shock genes, lowering transmission risk (Seah et al., 2021). The effect of dew point temperature remains inconclusive. A negative causal relationship may suggest that higher humidity inhibits mosquito flight, reducing transmission (Li et al., 2018). Conversely, a positive link implies that higher humidity extends mosquito lifespan and increases eclosion rates, promoting transmission (Thu et al., 1998). In summary, because the analysis framework proposed in this study reveals the nonlinear relationship between local meteorological elements and dengue fever transmission in Singapore, the final model is able to achieve better predictive performance.

Fig. 6 illustrates the schematic of the physical mechanisms by which climatic variables influence dengue fever in Singapore. It shows how key climatic variables affect dengue transmission. SST in three key regions influences local Singaporean climate by modulating large-scale atmospheric circulation, which in turn affects the activity of Aedes mosquitoes, the vectors for the dengue virus, and the replication of the virus, ultimately influencing the transmission of dengue fever in the Singaporean population. By capturing these physical mechanisms of how environmental factors at different scales affect dengue transmission, our model better predicts dengue under climate variability. The model proposed in this study, by considering multi-scale climatic factors such as SST and atmospheric circulation, achieves high accuracy, highlighting the importance of considering physical mechanisms in the modeling process.

4.2. Strengths and limitations

This study systematically analyzed the relationship and lagged causality between Singapore dengue cases and climate variables at different frequency scales from a novel perspective of time series decomposition. It clarified the mechanisms through which climate factors at various frequency scales influence dengue incidence in Singapore. Additionally, from a physical mechanism perspective, this study explored the influence of climate factors on dengue transmission, revealing how SST affects local meteorological variables by modulating atmospheric circulation, which in turn impacts the environment for dengue transmission. These results provide a new perspective for understanding the relationship between climate change and dengue transmission and offer theoretical and methodological support for future disease prediction and public health strategies.

Furthermore, the multi-scale short-term prediction model proposed by this study performed excellently in validation, demonstrating the significant impact of meteorological factors on dengue transmission in Singapore. Compared to the CNN-BiLSTM hybrid model used by Zhao et al. (2023), which is the most accurate weekly dengue prediction model publicly available, our model effectively captures the complex relationship between climate signals and dengue transmission and provides more precise predictions. Despite the model used by Zhao et al. (2023) having a Mean Absolute Percentage Error (MAPE) of 12.28 %, only 0.95 % lower than that of our study, this result indirectly supports the advantages of our model in terms of rationality and interpretability.

However, this study has some limitations. Firstly, it focused on the impact of climate variables on dengue transmission without fully considering other factors such as population growth, migration, government interventions, and urbanization, all of which can play important roles in shaping dengue dynamics (Struchiner et al., 2015). Socioeconomic drivers such as population size and economic development are likely to exert their influence over broader temporal scales (e.g., annual or multi-year trends), whereas at the weekly

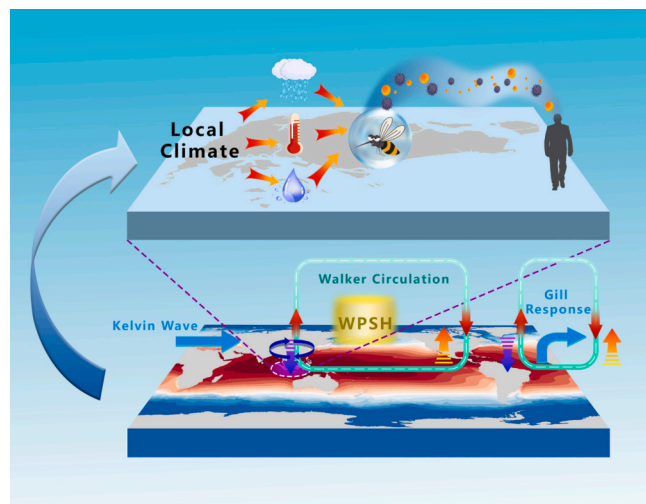


Fig. 6. Schematic of the physical mechanisms by which climate variables influence dengue transmission in Singapore. The ocean region is colored based on the mean SST from January 2012 to October 2016. "WPSH" represents the subtropical high, light green arrows indicate the Walker circulation, and the red arrows indicate the normal ascending or descending branches of the Walker circulation. Orange (dark blue) arrows indicate anomalies that suppress the Walker circulation's descending (ascending) branch. Blue arrows represent Kelvin waves excited by the Gill response, and blue circulations represent the anomalous circulation triggered by Kelvin waves in the region. (For interpretation of the references to colour in this figure legend, the reader is referred to the web version of this article.)

scale, short-term fluctuations in dengue transmission are more likely influenced by factors such as population mobility or intervention timing. But, fine-resolution data on mobility and interventions are often unavailable or inaccessible.

Secondly, in addition to the six climate variables analyzed, other climate factors such as air pressure, wind speed and finer scale meteorological variations may also affect dengue transmission in some locations. Studies in Guangzhou, China (Wang et al., 2014; Sang et al., 2014) reported associations between wind velocity, air pressure and dengue cases. However, the current evidence is geographically limited and often lacks clear mechanistic or biological explanations, especially when considered over larger regions and longer time periods.

Moreover, complex interactions between climatic and non-climatic factors, such as land-use changes, ecological shifts, or vector habitat modifications, may also influence dengue transmission dynamics but remain insufficiently understood. Recent studies have highlighted the combined effects of climate change, urbanization, and land-use transformation on the expansion of Aedes mosquito habitats and dengue risk (Messina et al., 2019). Insights from other fields, such as architecture and building energy optimization, demonstrate the value of integrating environmental and non-climatic variables to improve predictive performance (Naghipour et al., 2025; Naghipour and Naghipour, 2025a,b). Exploring these interactions is crucial for developing more comprehensive and mechanistically grounded predictive models, particularly under scenarios of rapid environmental change.

Thirdly, larger-scale climatic signals such as snow cover and sea ice may exert indirect or teleconnected effects on climate systems, which could in turn influence factors relevant to dengue vectors and transmission. However, for tropical and subtropical regions, SST in the tropical oceans—particularly the Indian Ocean—remains the primary climatic driver of dengue transmission (Chen et al., 2024). While snow cover and sea ice may affect tropical climates mainly through modulation of ocean temperatures rather than direct effects (Li et al., 2024), these high-latitude variables could become increasingly relevant as predictors in dengue risk models for higher-latitude regions where the habitat of Aedes mosquitoes is expanding.

Finally, this study is based on data from January 2012 to October 2016, with a limited sample size, which may constrain model complexity and generalizability. In addition, potential biases in the dengue case data, such as underreporting, delayed reporting, or misclassification, may affect model predictions. On the other hand, while our findings provide insights for Singapore, their applicability to other regions may be limited. Differences in climate, vector ecology, and population dynamics may require local calibration to maintain predictive accuracy.

Despite these limitations, the prediction modeling method proposed here has a strong theoretical foundation for analyzing the relationship between climate factors and dengue transmission. Even with a limited sample size and without considering certain socioeconomic factors, the model still effectively captures the complex relationship between climate signals and dengue transmission. Overall, this study not only provides a new analytical framework for understanding the impact of climate change on dengue transmission but also offers robust theoretical support for dengue prediction modeling, confirming the critical role of climate factors in the transmission process. Moreover, the insights gained from our modeling framework can inform public health interventions and early warning systems for dengue in Singapore. By identifying key climate drivers and their temporal patterns, decision-makers can better allocate vector control resources and plan timely interventions. With proper local calibration, this approach could also be adapted for use in other regions, enhancing the practical relevance of our study.

5. Conclusion

This study isolated pre-intervention dengue data from January 2012 to October 2016 in Singapore to avoid confounding by government control measures. Using CEEMDAN, we decomposed climate variables and dengue incidence into low-frequency, high-frequency, and trend components. Correlation analysis showed that low-frequency dengue variations were driven primarily by tropical Atlantic and Central Eastern Pacific SSTs, as well as local dew-point temperature, precipitation, and air temperature. High-frequency variations were dominated by Indian Ocean SST and local dew-point temperature. Trend changes reflected the combined influence of all six climate variables. PCMCI causality tests then confirmed that SSTs in these three regions modulate Singapore's meteorology through large-scale atmospheric circulation, thereby affecting Aedes activity, viral replication and ultimately dengue transmission. Building on these mechanistic insights, we developed and validated a short-term forecast model that effectively predicts dengue dynamics.

By elucidating how climate signals at distinct frequency scales drive dengue spread, our framework offers a physically grounded approach to disease prediction and early warning in the context of climate change. Future work should expand to other regions and longer time series to evaluate additional climate variables, such as air pressure, wind, snow cover, and sea ice. Moreover, incorporating high-resolution data on population mobility, intervention timing and other socioeconomic factors, when such data become available, would allow a more comprehensive assessment of the drivers of dengue transmission across temporal and spatial scales.

CRediT authorship contribution statement

Zhen Zhang: Writing – review & editing, Writing – original draft, Visualization, Validation, Software, Methodology, Data curation. **Shujuan Hu:** Writing – review & editing, Supervision, Resources, Funding acquisition, Conceptualization. **Jiaxuan Hu:** Writing – review & editing, Data curation. **Zihan Hao:** Writing – review & editing, Data curation. **Jianping Huang:** Writing – review & editing, Supervision, Project administration, Funding acquisition, Conceptualization.

Declaration of competing interest

The authors declare that they have no known competing financial interests or personal relationships that could have appeared to influence the work reported in this paper.

Acknowledgements

This work was supported by the National Key Research and Development Program of China (2023YFC3503400), the Self-supporting Program of Guangzhou Laboratory (SRPG22-007), the Special Program of Guangzhou National Laboratory (GZNL2024A01004).

Appendix A. Supplementary data

Supplementary data to this article can be found online at <https://doi.org/10.1016/j.ulim.2025.102734>.

Data availability

I have provided the data connection in the article.

References

Almeida, A.P., Baptista, S.S., Sousa, C.A., Novo, M.T., Ramos, H.C., Panella, N.A., Godsey, M., Simões, M.J., Anselmo, M.L., Komar, N., Mitchell, C.J., 2005. Bioecology and vectorial capacity of *Aedes albopictus* (Diptera: Culicidae) in Macao, China, in relation to dengue virus transmission. *J. Med. Entomol.* 42, 419–428. <https://doi.org/10.1093/jmedent/42.3.419>.

Anikeeva, O., Hansen, A., Varghese, B., Borg, M., Zhang, Y., Xiang, J., Bi, P., 2024. The impact of increasing temperatures due to climate change on infectious diseases. *BMJ* 387, e079343. <https://doi.org/10.1136/bmj-2024-079343>.

Appice, A., Gel, Y.R., Iliev, I., Lyubchich, V., Malerba, D., 2020. A multi-stage machine learning approach to predict dengue incidence: a case study in Mexico. *IEEE Access* 8, 52713–52725. <https://doi.org/10.1109/ACCESS.2020.2980634>.

Bhatt, S., Gething, P.W., Brady, O.J., Messina, J.P., Farlow, A.W., Moyes, C.L., Drake, J.M., Brownstein, J.S., Hoen, A.G., Sankoh, O., Myers, M.F., 2013. The global distribution and burden of dengue. *Nature* 496, 504–507. <https://doi.org/10.1038/nature12060>.

Chang, C.-P., Wang, Z., McBride, J., Liu, C.-H., 2005. Annual cycle of Southeast Asia—Maritime Continent rainfall and the asymmetric monsoon transition. *J. Clim.* 18 (2), 287–301. <https://doi.org/10.1175/JCLI-3257.1>.

Chen, Y., Xu, Y., Wang, L., Liang, Y., Li, N., Lourenço, J., Yang, Y., Lin, Q., Wang, L., Zhao, H., Cazelles, B., 2024. Indian Ocean temperature anomalies predict long-term global dengue trends. *Science* 384, 639–646. <https://doi.org/10.1126/science.adj4427>.

Choi, Y., Tang, C.S., McIver, L., Hashizume, M., Chan, V., Abeyasinghe, R.R., Iddings, S., Huy, R., 2016. Effects of weather factors on dengue fever incidence and implications for interventions in Cambodia. *BMC Public Health* 16, 1–7. <https://doi.org/10.1186/s12889-016-2923-2>.

Colón-González, F.J., Sewe, M.O., Tompkins, A.M., Sjödin, H., Casallas, A., Rocklöv, J., Caminade, C., Lowe, R., 2021. Projecting the risk of mosquito-borne diseases in a warmer and more populated world: a multi-model, multi-scenario intercomparison modelling study. *Lancet Planet. Health* 5, e404–e414.

Damtew, Y.T., Tong, M., Varghese, B.M., Anikeeva, O., Hansen, A., Dear, K., Zhang, Y., Morgan, G., Driscoll, T., Capon, T., Bi, P., 2023. Effects of high temperatures and heatwaves on dengue fever: a systematic review and meta-analysis. *EBioMedicine* 91. <https://doi.org/10.1016/j.ebiom.2023.104582>.

Dostal, T., Meissner, J., Munayco, C., García, P.J., Cárcamo, C., Pérez Lu, J.E., Morin, C., Frisbie, L., Rabinowitz, P.M., 2022. The effect of weather and climate on dengue outbreak risk in Peru, 2000–2018: a time-series analysis. *PLoS Neglect Trop Dis.* 16, e0010479. <https://doi.org/10.1371/journal.pntd.0010479>.

Earnest, A., Tan, S.B., Wilder-Smith, A., 2012. Meteorological factors and El Niño southern oscillation are independently associated with dengue infections. *Epidemiol. Infect.* 140, 1244–1251. <https://doi.org/10.1017/S095026881100183X>.

Gagnon, A.S., Bush, A.B., Smoyer-Tomic, K.E., 2001. Dengue epidemics and the El Niño southern oscillation. *Clim. Res.* 19, 35–43. <https://doi.org/10.3354/cr019035>.

García-Carreras, B., Yang, B., Grabowski, M.K., Sheppard, L.W., Huang, A.T., Salje, H., Clapham, H.E., Iamsirithaworn, S., Doung-Ngern, P., Lessler, J., Cummings, D.A., 2022. Periodic synchronisation of dengue epidemics in Thailand over the last 5 decades driven by temperature and immunity. *PLoS Biol.* 20 (3), e3001160. <https://doi.org/10.1371/journal.pbio.3001160>.

H2O.ai, 2023a. H2O AutoML: Automated Machine Learning for Everyone. <https://docs.h2o.ai/h2o/latest-stable/h2o-docs/automl.html> (accessed 5 March 2023).

H2O.ai, 2023b. H2O-3: Open Source Distributed Machine Learning Platform. <https://github.com/h2oai/h2o-3> (accessed 5 March 2023).

Ho, S.H., Lim, J.T., Ong, J., Japuarachchi, H.C., Sim, S., Ng, L.C., 2023. Singapore's 5 decades of dengue prevention and control—implications for global dengue control. *PLoS Neglect Trop Dis.* 17, e0011400. <https://doi.org/10.1371/journal.pntd.0011400>.

Huey, R.B., Stevenson, R.D., 1979. Integrating thermal physiology and ecology of ectotherms: a discussion of approaches. *Am. Zool.* 19, 357–366. <https://doi.org/10.1093/icb/19.1.357>.

Jayasani, C., Dammalage, P., Sarathchandra, S., Godaliyadda, R., Ekanayake, P., Herath, V., Ekanayake, J., Dharmaratne, S., 2021. Limited data forecasting for dengue propagation. In: 2021 10th International Conference on Information and Automation for Sustainability (ICIAfs). IEEE, pp. 416–421. <https://doi.org/10.1109/ICIAfs52090.2021.9606032>.

Kakarla, S.G., Kondeti, P.K., Vavilala, H.P., Boddeda, G.S., Mopuri, R., Kumaraswamy, S., Kadiri, M.R., Mutheneni, S.R., 2023. Weather integrated multiple machine learning models for prediction of dengue prevalence in India. *Int. J. Biometeorol.* 67, 285–297. <https://doi.org/10.1007/s00484-022-02405-z>.

Kok, B.H., Lim, H.T., Lim, C.P., Lai, N.S., Leow, C.Y., Leow, C.H., 2023. Dengue virus infection—a review of pathogenesis, vaccines, diagnosis and therapy. *Virus Res.* 324, 199018. <https://doi.org/10.1016/j.virusres.2022.199018>.

Kraemer, M.U., Reiner Jr., R.C., Brady, O.J., Messina, J.P., Gilbert, M., Pigott, D.M., Yi, D., Johnson, K., Earl, L., Marczak, L.B., Shirude, S., 2019. Past and future spread of the arbovirus vectors *Aedes aegypti* and *Aedes albopictus*. *Nat. Microbiol.* 4, 854–863. <https://doi.org/10.1038/s41564-019-0376-y>.

Li, C., Lu, Y., Liu, J., Wu, X., 2018. Climate change and dengue fever transmission in China: evidences and challenges. *Sci. Total Environ.* 622, 493–501. <https://doi.org/10.1016/j.scitotenv.2017.11.326>.

Li, X., Zhang, J., Fang, X., et al., 2024. Reduction in Arctic sea ice amplifies the warming of the northern Indian Ocean. *Atmos Res.* 312, 107763. <https://doi.org/10.1016/j.atmosres.2024.107763>.

Lim, J.T., Chew, L.Z., Choo, E.L., Dickens, B.S., Ong, J., Aik, J., Ng, L.C., Cook, A.R., 2021. Increased dengue transmissions in Singapore attributable to SARS-CoV-2 social distancing measures. *J. Infect. Dis.* 223, 399–402. <https://doi.org/10.1093/infdis/jiaa619>.

Liu, Y., Wang, X., Tang, S., Cheke, R.A., 2023. The relative importance of key meteorological factors affecting numbers of mosquito vectors of dengue fever. *PLoS Neglect Trop Dis.* 17, e0011247. <https://doi.org/10.1371/journal.pntd.0011247>.

Liu-Helmersson, J., Stenlund, H., Wilder-Smith, A., Rocklöv, J., 2014. Vectorial capacity of *Aedes aegypti*: effects of temperature and implications for global dengue epidemic potential. *PLoS One* 9, e89783. <https://doi.org/10.1371/journal.pone.0089783>.

Liu-Helmersson, J., Quam, M., Wilder-Smith, A., Stenlund, H., Ebi, K., Massad, E., Rocklöv, J., 2016. Climate change and *Aedes* vectors: 21st century projections for dengue transmission in Europe. *EBioMedicine* 7, 267–277. <https://doi.org/10.1016/j.ebiom.2016.03.046>.

Lowe, R., Barcellos, C., Coelho, C.A., Bailey, T.C., Coelho, G.E., Graham, R., Jupp, T., Ramalho, W.M., Carvalho, M.S., Stephenson, D.B., Rodó, X., 2014. Dengue outlook for the world cup in Brazil: an early warning model framework driven by real-time seasonal climate forecasts. *Lancet Infect. Dis.* 14, 619–626. [https://doi.org/10.1016/S1473-3099\(14\)70781-9](https://doi.org/10.1016/S1473-3099(14)70781-9).

Lu, L., Lin, H., Tian, L., Yang, W., Sun, J., Liu, Q., 2009. Time series analysis of dengue fever and weather in Guangzhou, China. *BMC Public Health* 9, 1–5. <https://doi.org/10.1186/1471-2458-9-395>.

Messina, J.P., Brady, O.J., Golding, N., Kraemer, M.U.G., Wint, G.R.W., Ray, S.E., Pigott, D.M., Shearer, F.M., Johnson, K., Earl, L., Marczak, L.B., Shirude, S., Weaver, N.D., Gilbert, M., Velayudhan, R., Jones, P., Jaenisch, T., Scott, T.W., Reiner Jr., R.C., Hay, S.I., 2019. The current and future global distribution and population at risk of dengue. *Nat. Microbiol.* 4 (9), 1508–1515. <https://doi.org/10.1038/s41564-019-0476-8>.

Messina, J.P., Brady, O.J., Scott, T.W., Zou, C., Pigott, D.M., Duda, K.A., Bhatt, S., Katzenback, L., Howes, R.E., Battle, K.E., Simmons, C.P., 2014. Global spread of dengue virus types: mapping the 70 year history. *Trends Microbiol.* 22, 138–146. <https://doi.org/10.1016/j.tim.2013.12.011>.

Ministry of Health Singapore (MOH), 2023. Weekly Infectious Diseases Bulletin 2023. <https://www.moh.gov.sg> (accessed 3 April 2023).

Naghipour, P., Naghipour, A., 2025a. Energy performance analysis of residential buildings in Bandar Anzali: Influence of orientation and aspect ratio. *Next Sustain* 5, 100140. <https://doi.org/10.1016/j.nxust.2025.100140>.

Naghipour, P., Naghipour, A., 2025b. Evaluating heating energy consumption in residential buildings using hybrid machine learning models: the case of parsabad city. *Next Res.* 2, 100721. <https://doi.org/10.1016/j.nexres.2025.100721>.

Naghipour, P., Naghipour, A., Shirdel, A.H., et al., 2025. Sustainability in historical Islamic architecture: lessons from Sheikh Lotfollah Mosque's construction techniques. *J. Islamic Archit.* 8, 585–603. <https://doi.org/10.18860/jia.v8i3.29053>.

Nakhapakorn, K., Tripathi, N.K., 2005. An information value based analysis of physical and climatic factors affecting dengue fever and dengue haemorrhagic fever incidence. *Int. J. Health Geogr.* 4, 1–3. <https://doi.org/10.1186/1476-072X-4-13>.

National Oceanic and Atmospheric Administration (NOAA), 2023. Hourly Meteorological Data for Seletar Airport and Changi Airport, Singapore. <https://www.ncei.noaa.gov/maps/hourly> (accessed 23 March 2024).

National Oceanic and Atmospheric Administration (NOAA) Physical Sciences Laboratory (PSL), 2023. Global Weekly Sea Surface Temperature Data. <https://psl.noaa.gov> (accessed 23 March 2024).

Project Wolbachia-Singapore Consortium, Ching, N.L., 2021. Wolbachia-Mediated Sterility Suppresses *Aedes Aegypti* Populations in the Urban Tropics. *MedRxiv*. <https://doi.org/10.1101/2021.06.16.21257922>, 2021–06.

Reinhold, J.M., Lazzari, C.R., Lahondère, C., 2018. Effects of the environmental temperature on *Aedes aegypti* and *Aedes albopictus* mosquitoes: a review. *Insects* 9, 158. <https://doi.org/10.3390/insects9040158>.

Rong, X., Zhang, R., Li, T., 2010. Impacts of Atlantic Sea surface temperature anomalies on Indo-east Asian summer monsoon-ENSO relationship. *Chin. Sci. Bull.* 55, 2458–2468. <https://doi.org/10.1007/s11434-010-3098-3>.

Runge, J., Nowack, P., Kretschmer, M., Flaxman, S., Sejdinovic, D., 2019. Detecting and quantifying causal associations in large nonlinear time series datasets. *Sci. Adv.* 5, eaau4996. <https://doi.org/10.1126/sciadv.aau4996>.

Sang, S., Yin, W., Bi, P., Zhang, H., Wang, C., Liu, X., et al., 2014. Predicting local dengue transmission in Guangzhou, China, through the influence of imported cases, mosquito density and climate variability. *PLoS ONE* 9, e102755. <https://doi.org/10.1371/journal.pone.0102755>.

Seah, A., Aik, J., Ng, L.C., Tam, C.C., 2021. The effects of maximum ambient temperature and heatwaves on dengue infections in the tropical city-state of Singapore—a time series analysis. *Sci. Total Environ.* 775, 145117. <https://doi.org/10.1016/j.scitotenv.2021.145117>.

Seidahmed, O.M., Eltahir, E.A., 2016. A sequence of flushing and drying of breeding habitats of *Aedes aegypti* (L.) prior to the low dengue season in Singapore. *PLoS Neglect Trop Dis.* 10, e0004842. <https://doi.org/10.1371/journal.pntd.0004842>.

Souza, C.D.F., Nascimento, R.P.D.S., Bezerra-Santos, M., Armstrong, A.D.C., Gomes, O.V., Nicácio, J.M., 2024. Silva Júnior JVJ, do Carmo RF. Space-time dynamics of the dengue epidemic in Brazil, 2024: an insight for decision making. *BMC Infect Dis* 24, 1056. <https://doi.org/10.1186/s12879-024-09813-z>.

Spirites, P., Glymour, C., 1991. An algorithm for fast recovery of sparse causal graphs. *Soc. Sci. Comput. Rev.* 9, 62–72.

Struchiner, C.J., Rocklöv, J., Wilder-Smith, A., Massad, E., 2015. Increasing dengue incidence in Singapore over the past 40 years: population growth, climate and mobility. *PLoS One* 10, e0136286. <https://doi.org/10.1371/journal.pone.0136286>.

Thu, H.M., Aye, K.M., Thein, S., 1998. The effect of temperature and humidity on dengue virus propagation in *Aedes aegypti* mosquitos. *Southeast Asian J. Trop. Med. Public Health* 29, 280–284.

Torres, M.E., Colominas, M.A., Schlotthauer, G., Flandrin, P., 2011. A complete ensemble empirical mode decomposition with adaptive noise. In: 2011 IEEE International Conference on Acoustics, Speech and Signal Processing (ICASSP). IEEE, pp. 4144–4147. <https://doi.org/10.1109/ICASSP.2011.5947265>.

Truong, A., Walters, A., Goodlett, J., Hines, K., Bruss, C.B., Farivar, R., 2019. Towards automated machine learning: Evaluation and comparison of AutoML approaches and tools. In: 2019 IEEE 31st International Conference on Tools with Artificial Intelligence (ICTAI). IEEE, pp. 1471–1479. <https://doi.org/10.1109/ICTAI.2019.000209>.

Van Panhuis, W.G., Choisy, M., Xiong, X., Chok, N.S., Akarasewi, P., Iamsirithaworn, S., Lam, S.K., Chong, C.K., Lam, F.C., Phommasak, B., Vongphrachanh, P., 2015. Region-wide synchrony and traveling waves of dengue across eight countries in Southeast Asia. *Proc. Natl. Acad. Sci. USA* 112 (42), 13069–13074. <https://doi.org/10.1073/pnas.1501375112>.

Wang, C., Jiang, B., Fan, J., Wang, F., Liu, Q., 2014. A study of the dengue epidemic and meteorological factors in Guangzhou, China, by using a zero-inflated Poisson regression model. *Asia Pac. J. Public Health* 26, 48–57. <https://doi.org/10.1177/1010539513490195>.

Wilder-Smith, A., Gubler, D.J., 2008. Geographic expansion of dengue: the impact of international travel. *Med. Clin. North Am.* 92, 1377–1390. <https://doi.org/10.1016/j.mcna.2008.07.002>.

World Health Organization (WHO), 2023. Geographical Expansion of Cases of Dengue and Chikungunya Beyond the Historical Areas of Transmission in the Region of the Americas. [https://www.who.int/emergencies/diseases-outbreak-news/item/2023-DON448#:~:text=During%20the%20same%20period%2C%20the,100%20000%20population%20\(3](https://www.who.int/emergencies/diseases-outbreak-news/item/2023-DON448#:~:text=During%20the%20same%20period%2C%20the,100%20000%20population%20(3) (accessed 23 March 2024).

World Health Organization (WHO), 2023. Dengue and severe dengue. WHO fact sheet (accessed 25 September 2025). <https://www.who.int/news-room/fact-sheets/detail/dengue-and-severe-dengue>.

Xiao, F.Z., Zhang, Y., Deng, Y.Q., He, S., Xie, H.G., Zhou, X.N., Yan, Y.S., 2014. The effect of temperature on the extrinsic incubation period and infection rate of dengue virus serotype 2 infection in *Aedes albopictus*. *Arch. Virol.* 159, 3053–3057. <https://doi.org/10.1007/s00705-014-2051-1>.

Yang, X., Quam, M.B., Zhang, T., Sang, S., 2021. Global burden for dengue and the evolving pattern in the past 30 years. *J. Travel Med.*, taab146 <https://doi.org/10.1093/jtm/taab146>.

Yoo, S.H., Yang, S., Ho, C.H., 2006. Variability of the Indian Ocean Sea surface temperature and its impacts on Asian-Australian monsoon climate. *J. Geophys. Res.-Atmos.* 111. <https://doi.org/10.1029/2005JD006001>.

Zhao, X., Li, K., Ang, C.K., Cheong, K.H., 2023. A deep learning based hybrid architecture for weekly dengue incidences forecasting. *Chaos, Solitons Fractals* 168, 113170. <https://doi.org/10.1016/j.chaos.2023.113170>.